

Published in final edited form as:

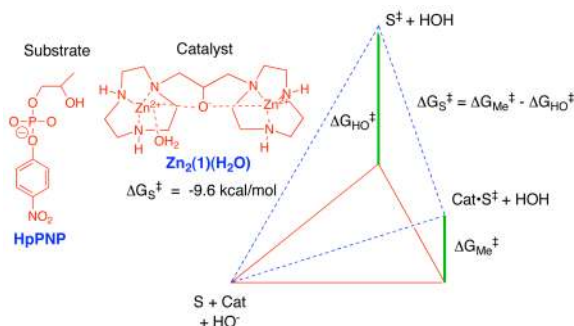
Acc Chem Res. 2008 April ; 41(4): 539–548. doi:10.1021/ar7002013.

Phosphate Binding Energy and Catalysis by Small and Large Molecules

Janet R. Morrow, Tina L. Amyes, and John P. Richard*

Department of Chemistry, University at Buffalo, SUNY, Buffalo, NY 14260-3000

Conspectus



Catalysis is an important process in chemistry and enzymology. The rate acceleration for any catalyzed reaction is the difference between the activation barriers for the uncatalyzed ($\Delta G_{\text{HO}}^{\ddagger}$) and catalyzed ($\Delta G_{\text{Me}}^{\ddagger}$) reactions, which corresponds to the binding energy ($\Delta G_{\text{S}}^{\ddagger} = \Delta G_{\text{Me}}^{\ddagger} - \Delta G_{\text{HO}}^{\ddagger}$) for transfer of the reaction transition state from solution to the catalyst. This transition state binding energy is a fundamental descriptor of catalyzed reactions, and its evaluation is necessary for an understanding of any and all catalytic processes.

We have evaluated the transition state binding energies obtained from interactions between low molecular weight metal ion complexes or high molecular weight protein catalysts and the phosphate group of bound substrate. Work on catalysis by small molecules is exemplified by studies on the mechanism of action of $\text{Zn}_2(1)(\text{H}_2\text{O})$. A binding energy of $\Delta G_{\text{S}}^{\ddagger} = -9.6$ kcal/mol was determined for $\text{Zn}_2(1)(\text{H}_2\text{O})$ -catalyzed cleavage of the RNA analog **HpPNP**. The pH-rate profile for this cleavage reaction showed that there is optimal catalytic activity at high pH, where the catalyst is in the basic form $[\text{Zn}_2(1)(\text{HO}^-)]$. However, it was also shown that the active form of the catalyst is $\text{Zn}_2(1)(\text{H}_2\text{O})$, and that this recognizes the C2-oxygen-ionized substrate in the cleavage reaction. The active catalyst $\text{Zn}_2(1)(\text{H}_2\text{O})$ shows a high affinity for oxyphosphorane transition state dianions and a stable methyl phosphate transition state analog, compared with the affinity for phosphate monoanion substrates. The transition state binding energies $\Delta G_{\text{S}}^{\ddagger}$ for cleavage of **HpPNP** catalyzed by a variety Zn^{2+} and Eu^{3+} metal ion complexes reflect the increase in the catalytic activity with the total positive charge at the catalyst. These values of $\Delta G_{\text{S}}^{\ddagger}$ are affected by interactions between the metal ion and its ligands, but these effects are small in comparison with $\Delta G_{\text{S}}^{\ddagger}$ observed for catalysis by free metal ions, where the ligands are water.

Enzymes are unique in having evolved mechanisms to effectively utilize binding interactions with nonreacting fragments of the substrate in stabilization of the reaction transition state. Orotidine 5'-

EMAIL: jrichard@chem.buffalo.edu.

Janet R. Morrow received a B.S. degree in chemistry from the University of California, Santa Barbara and her Ph.D. degree in Chemistry from the University of North Carolina, Chapel Hill. She is currently Professor of Chemistry at the University at Buffalo, SUNY.

Biographies for Tina L. Amyes and John P. Richard were published in an earlier issue of *Accounts of Chemical Research*.

monophosphate decarboxylase, α -glycerol phosphate dehydrogenase and triosephosphate isomerase catalyze dissimilar decarboxylation, hydride transfer and proton transfer reactions, respectively. Each enzyme derives ca. 12 kcal/mol of transition state stabilization from protein interactions with the nonreacting phosphate group, which is larger than the highest ≈ 10 kcal/mol transition state stabilization that we have determined for small-molecule catalysis of phosphate diester cleavage in water. Each of these enzymes catalyze the slow reaction of a truncated substrate that lacks the phosphate group, and in each case the reaction of the truncated substrate is strongly activated by the *allosteric* binding of the second substrate “piece” phosphite dianion, HPO_3^{2-} . We propose a modular design for these enzymes with a classical active site which recognizes the reactive substrate fragment, and a separate phosphodianion binding site. The second site is created, in part, by flexible protein loops that wrap around the substrate phosphodianion group and *bury* the substrate in an environment with an optimal local dielectric constant for the catalyzed reaction, and with the most favorable positioning of the catalytic side chains. This design is easily generalized to a wide variety of enzyme-catalyzed reactions.

Linus Pauling noted that catalysis in general, and by enzymes in particular, will result from the development of tight interactions between the catalyst and the transition state for the catalyzed reaction.¹ This is shown by the transition state binding energy ΔG_S^\ddagger (Scheme 1). Catalysis by most enzymes is so efficient that release of products would be strongly rate-determining, if they were to bind with the same affinity as the transition state. Consequently, enzymes show a large discrimination and bind their substrates/products much more weakly than the reaction transition state (Scheme 1).²

The Pauling paradigm has a particular appeal when trying to explain catalysis to students. On the other hand, there are issues that must be addressed if this model is to be accepted as a starting framework for explaining enzyme catalysis. These include:

1. Recently, Zhang and Houk wrote: “While complementarity of the type proposed by Pauling can account for acceleration up to 11 orders of magnitude, most enzymes exceed that proficiency”.³ They therefore proposed that enzymes “achieve over 15 kcal/mol of *transition state binding* not merely by a concatenation of noncovalent effects but by covalent bond formation between enzyme or cofactor and transition state, involving a change in mechanism from that in aqueous solution”.³
2. There are only small differences in the structure of the substrate/product and the transition state for many enzyme-catalyzed reactions. The origin of the large differential binding of these species is generally unknown.²
3. Enzymes are large molecules that undergo many types of motion, some of which may be coupled to catalysis. Further, catalysis of chemical reactions must ultimately be explained at the level of quantum mechanics. Since neither protein dynamics nor quantum mechanics are central to the Pauling paradigm, more sophisticated models for catalysis might either use this paradigm as a starting point, as a specialized example or, in the most extreme case, discard it entirely.

Our goal as experimentalists has been to characterize the mechanisms for catalysis by small metal ion complexes, and by larger enzymes where much or all of the catalytic power is derived from the utilization of phosphate binding energy. We summarize here the results of this work, and provide an interpretation of our results within the framework of the Pauling model.

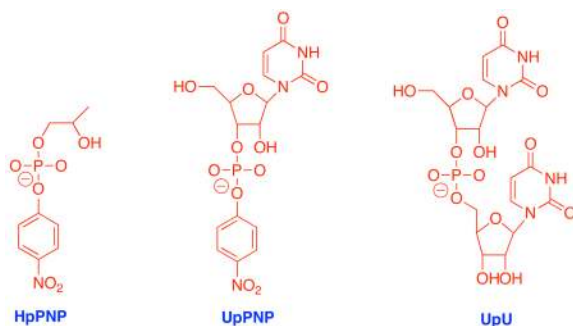
Phosphate Diester Cleavage

The design of catalysts to cleave RNA has considerable intellectual appeal, along with potential to produce RNA cleavage reagents that have practical applications.^{4–6} JRM has shown that lanthanide(III) complexes are efficient catalysts of the cleavage of RNA,^{7,8} and she has

examined cleavage of the 5' cap of *m*RNA by several metal ion-macrocycle complexes.⁹ Recent collaborative work between the Morrow and Richard laboratories has focused on characterizing the rate acceleration for catalysis by metal ion complexes and defining the origin of the catalytic rate acceleration.

Kinetic Analyses

An examination of the literature suggested to us that the laboratory time expended in the synthesis of novel metal ion catalysts of RNA cleavage often exceeded the time spent in characterizing their kinetics and mechanism of action. In particular, it is difficult to compare the catalytic activity of metal ion complexes prepared in different laboratories, because there is no commonly agreed upon protocol for measuring and reporting the kinetic parameters for catalysis. Our initial goal was to develop such a protocol for reporting kinetic data for metal ion complex-catalyzed phosphate diester cleavage in water at 25 °C, in the hope that it might be adopted by other laboratories.



We have reported second-order rate constants k_{Me} for the catalyzed cleavage of **HpPNP**, **UpPNP** and **UpU** to form cyclic phosphate diesters. These rate constants are generally determined as the slopes of linear plots of k_{obsd} (s^{-1}) for phosphate diester cleavage against the catalyst concentration. The rate constant k_{Me} has the same units ($M^{-1} s^{-1}$) and meaning as k_{cat}/K_m for an enzyme-catalyzed reaction. Values of k_{Me} determined at Buffalo and elsewhere can be directly compared in order to provide a simple and meaningful measure of the catalytic activity of different metal ion complexes, or of their activity relative to enzyme catalysts.

The catalytic effectiveness of a variety of metal ion complexes was then evaluated over a broad range of pH. Figure 1 shows representative pH-rate profiles for the **Zn₂(1)(H₂O)-** and **Zn(2) H₂O-**catalyzed cleavage of **HpPNP**, and for the spontaneous specific-base-catalyzed cleavage of **HpPNP**.¹⁰ These profiles show that the *complex* between **HpPNP** and the fully protonated catalyst is inactive and that this complex is converted to the active form upon loss of a proton. Maximal activity is observed at high pH, where the metal-bound water of the free catalyst is ionized. The pH- and pD-rate profiles for catalysis of the cleavage of **HpPNP**, **UpPNP** and **UpU** by a broad range of mono- and dinuclear catalysts are also governed by ionization of a metal-bound water, as shown in Scheme 2.^{10–19} The data in Figure 1 and for related catalyzed reactions show a good fit to eq 1 derived for Scheme 2, using the values of K_a determined by potentiometric titration.¹⁰



$$k_{\text{Me}} = \left[\frac{k_{\text{Zn}} K_{\text{a}}}{K_{\text{a}} + [\text{H}^+]} \right] \quad (1)$$

Figure 1 shows that the relative activity of **Zn₂(1)(H₂O)** and **Zn(2)(H₂O)** as catalysts of the cleavage of **HpPNP** depends upon whether the observed second-order rate constants k_{Me} are compared at high or low pH. There is only a 12-fold difference in the *apparent* reactivity of the ionized dinuclear complex **Zn₂(1)(H₂O)** and the mononuclear complex **Zn(2)(H₂O)** at high pH. This difference increases to 290-fold for reactions at low pH because the downward break in catalytic activity is observed at a higher pH for **Zn(2)(H₂O)**, as a result of the 1.2 unit higher $\text{p}K_{\text{a}}$ for ionization of the zinc-bound water at **Zn(2)(H₂O)** than of that at **Zn₂(1)(H₂O)**.¹⁰

The high catalytic activity of **Zn₂(1)(H₂O)** is notable, because tethering two mononuclear Zn^{2+} complexes to form a dinuclear complex often causes only a statistical ca. 2-fold increase in catalytic activity.¹⁵ The X-ray structure of crystals (grown at pH 6.0) of the perchlorate salt of **Zn₂(1)(H₂O)** shows that the two Zn^{2+} are separated by only 3.66 Å, due to shielding of the electrostatic interaction between the metal cations by the bridging alkoxide.¹⁰ The interactions between the two Zn^{2+} and the linker alkoxide anion draw the metal cations into a densely-charged core, which provides a particularly large electrostatic stabilization of the dianionic transition state for phosphate diester cleavage.^{10,15}

$$\Delta G_{\text{S}}^{\ddagger} = \Delta G_{\text{Me}}^{\ddagger} - \Delta G_{\text{HO}}^{\ddagger} = -RT \ln \left[\frac{k_{\text{Zn}} K_{\text{a}} / K_{\text{w}}}{k_{\text{HO}}} \right] \quad (2)$$

Transition State Binding Energies

Our next goal was to obtain a simple measure of catalytic effectiveness from our kinetic data. The rate accelerations for the catalyzed cleavage of **HpPNP**, given by eq 2 derived for Scheme 3, were calculated from the relative displacement of the parallel lines for the formally HO^- -catalyzed cleavage (◆, Figure 1) and the HO^- -dependent metal ion complex-catalyzed reactions (● and ■), where K_{a} is the ionization constant for the metal-bound water and $K_{\text{w}} = 10^{-14} \text{ M}^2$.²⁰ The transition state binding energies of $\Delta G_{\text{S}}^{\ddagger} = -9.6$ and -6.3 kcal/mol for the reactions catalyzed by **Zn₂(1)(H₂O)** ($K_{\text{a}} = 10^{-7.8} \text{ M}$) and **Zn(2)(H₂O)** ($K_{\text{a}} = 10^{-9.2} \text{ M}$) respectively, correspond to 1.1×10^7 -fold and 4×10^7 -fold rate accelerations over the specific-base-catalyzed reaction.¹⁰ **Zn₂(1)(H₂O)** is an extremely impressive small molecule catalyst. Metal ion complexes with even higher catalytic activity in water,²¹ and in methanol²² have been prepared.

Figure 2 shows the transition state binding energy as the difference in the activation barrier for HO^- -catalyzed cleavage of an RNA analog and for the metal ion complex-catalyzed reaction, which is also an HO^- -dependent reaction (eq 2). The calculation of $\Delta G_{\text{S}}^{\ddagger}$ compresses extensive kinetic data into a single parameter that provides a direct measure for catalytic activity at neutral pH, where the catalyst is largely protonated. We have determined the values of $\Delta G_{\text{S}}^{\ddagger}$ for a wide variety of metal ion complex-catalyzed reactions and used these data to evaluate the effect of changing catalyst and substrate structure on catalytic activity.^{11,14,16,18–20}

Active Form of Catalyst

The pH dependence (Figure 1) of the uncatalyzed and catalyzed cleavage of **HpPNP** at $\text{pH} < (\text{catalyst } \text{p}K_{\text{a}})$ shows that under these conditions a proton is lost from the catalyst or substrate

on proceeding to the rate-determining transition state. This kinetic analysis cannot distinguish between: (a) the loss of proton from the substrate, in which case $\text{Zn}_2(1)(\text{H}_2\text{O})$ is the active catalyst; and, (b) the loss of a proton from the catalyst, in which case the active form of the catalyst is $\text{Zn}_2(1)(\text{HO}^-)$, whose concentration approaches a limit at $\text{pH} > \text{pK}_a$ (Scheme 2).^{10,12}

Analysis of inhibition of the $\text{Zn}_2(1)(\text{H}_2\text{O})$ -catalyzed cleavage of **HpPNP** shows that methylphosphate dianion binds to $\text{Zn}_2(1)(\text{H}_2\text{O})$ with a 1600-fold higher affinity than does diethylphosphate monoanion.²³ This strong and specific binding of the stable dianion resembles the specific binding of the dianionic transition state for cleavage of **HpPNP** to $\text{Zn}_2(1)(\text{H}_2\text{O})$, with an affinity that is much greater than that of the substrate monoanion.¹⁰ We concluded that methyl phosphate dianion is a transition state analog for the $\text{Zn}_2(1)(\text{H}_2\text{O})$ -catalyzed cleavage of phosphate diesters.²⁴

Apparent inhibition constants K_i for inhibition of $\text{Zn}_2(1)(\text{H}_2\text{O})$ -catalyzed cleavage of **HpPNP** by methyl phosphate dianion approach a limiting small value of 6×10^{-6} M for formation of a tight complex at low pH, where the catalyst exists mainly in the protonated form $\text{Zn}_2(1)(\text{H}_2\text{O})$.²³ These data (not shown) were fit to the model in Scheme 4 in which the transition state *analog* dianion binds to the active protonated catalyst $\text{Zn}_2(1)(\text{H}_2\text{O})$ but not to the ionized catalyst $\text{Zn}_2(1)(\text{HO}^-)$. We concluded that $\text{Zn}_2(1)(\text{H}_2\text{O})$ is the active catalyst that stabilizes the transition state dianion, and that it is converted to the inactive form $\text{Zn}_2(1)(\text{HO}^-)$ when the pH is increased above $\text{pK}_a = 7.8$. Deprotonation of $\text{Zn}_2(1)(\text{H}_2\text{O})$ may inactivate the catalyst by changing the favorable displacement of the water ligand by the substrate phosphate monoanion to an unfavorable reaction for the displacement of the strongly basic hydroxide ion ligand.

A change in solvent from H_2O to D_2O causes an increase from 7.8 to 8.4 in the pK_a of the zinc-bound water at $\text{Zn}_2(1)(\text{L}_2\text{O})$ (Scheme 2), but has little effect on the reactivity of $\text{Zn}_2(1)(\text{L}_2\text{O})$ towards cleavage of **UpPNP**.¹² Therefore, there is no primary kinetic solvent deuterium isotope effect on the cleavage reaction that results from movement of a hydron in the rate-determining transition state,¹² such as occurs in reactions where there is concerted general base catalysis (GBC, Scheme 5A). We concluded that the phosphate diester cleavage reaction follows the specific-base-catalyzed (SBC) pathway shown in Scheme 5B.

We have proposed that the SBC pathway is observed for catalysis by these metal ion complexes because of the dominant role played by electrostatics in stabilization of the transition state for cleavage of RNA analogues by interactions with the metal ion complex catalyst (Scheme 5B).¹² In other words, that the “covalent”-type stabilization *gained* by placing the Brønsted base at the transition state for the GBC reaction (Scheme 5A) is smaller than the electrostatic stabilization *lost* upon partial neutralization of negative charge at the now partly protonated O-2.

Structure-Reactivity Effects

We next used the above kinetic protocols to examine the effect of systematic changes in the metal cation, ligand and substrate structure on the transition state binding energy ΔG_S^\ddagger (Scheme 3) for reactions catalyzed by free metal ions and by metal ion complexes.

Ligand Effects

Chart 1 shows transition state binding energies (ΔG_S^\ddagger , Scheme 3) for catalysis of the cleavage of **HpPNP** by several mononuclear Zn^{2+} complexes, and by hydrated Zn^{2+} .¹⁸ By comparison, a value of $\Delta G_S^\ddagger = -3.3$ kcal/mol was determined for Zn^{2+} -catalyzed deprotonation of acetone,²⁵ where Zn^{2+} interacts with a monoanionic rather than a dianionic transition state. A value

of $\Delta G_S^\ddagger = -6.1$ kcal/mol was determined for Zn^{2+} -catalyzed aldose-ketose isomerization of trioses, where there is additional stabilization of the transition state from a *chelate* effect (Scheme 6).²⁶

Zn^{2+} alone is a good catalyst of the cleavage of **HpPNP** (Chart 1). However, it is not possible to obtain large rate constants for this catalyzed cleavage at high pH, because of the sparing solubility of hydrated Zn^{2+} . Ligands **2–5** strongly enhance catalysis by increasing the total concentration of soluble metal cation. The small variation in ΔG_S^\ddagger across Chart 1 suggests a similar origin for the transition state stabilization, which we propose is mainly stabilizing electrostatic interactions between the metal cation and transition state dianion.¹⁸

Chart 1 shows that macrocycle ligands either increase or decrease the catalytic activity compared to the case where there is no ligand, but that the effect on ΔG_S^\ddagger is ≤ 1 kcal/mol. The formation of Zn^{2+} complexes has the effect of shifting positive charge from Zn^{2+} to the electron-donor ligand atom, so that the weakest complexes will tend to show the highest charge density at Zn^{2+} . The complexes of Zn^{2+} to macrocycles **4** and **5** are substantially weaker than the complexes to **2** and **3**, but the weakly bound Zn^{2+} at the former complexes shows the greater catalytic activity (Chart 1).¹⁸ The higher activity of **Zn(4)(H₂O)** and **Zn(5)(H₂O)** may due to the larger positive charge density at the more weakly coordinated Zn^{2+} , and the resulting enhancement of stabilization from electrostatic interactions with the dianionic transition state.¹⁸

Cation Effects

The second-order rate constants for cleavage of **HpPNP** catalyzed by **Cu₂(1)(H₂O)** (Chart 2) are much smaller than those for catalysis by **Zn₂(1)(H₂O)** under the same conditions, and are invariant between pH 7 and 10.¹⁴ The X-ray crystal structure for **Cu₂(1)(H₂O)** shows a bridging alkoxide linker and a Cu(II)-Cu(II) distance of 3.58 Å,²⁷ similar to that observed in the crystal structure for **Zn₂(1)(H₂O)**.¹⁰ The structure for **Zn₂(1)(H₂O)** shows one hexacoordinated and one pentacoordinated Zn(II),¹⁰ while the structure for **Cu₂(1)(H₂O)** shows two pentacoordinated Cu(II).²⁷ We proposed that the coordination site missing from **Cu₂(1)(H₂O)** is essential for the efficient binding and catalysis of the reaction **HpPNP**.

The larger absolute transition state binding energy of $|\Delta G_S^\ddagger| = 9.8$ kcal/mol for cleavage of **HpPNP** catalyzed by Eu(III) (mainly $[\text{Eu}(\text{OH}_2)_9]^{3+}$)¹⁹ in water than for cleavage catalyzed by hydrated Zn^{2+} in water ($|\Delta G_S^\ddagger| = 6.6$ kcal/mol, Chart 1)¹⁸ is probably due to the stronger stabilizing electrostatic interaction of a trication than of a dication with the transition state dianion. Chart 3 gives the values of ΔG_S^\ddagger for catalysis of cleavage of **HpPNP** by mononuclear Eu(III) complexes to **6**¹⁶ and **7**,¹⁹ and for a dinuclear complex that forms by spontaneous dimerization of $[\text{Eu}(\text{6})(\text{OH}_2)_2]^+$ at pH ≥ 7.5 .¹⁶

The value of $|\Delta G_S^\ddagger| = 8.6$ kcal/mol for catalysis by $[\text{Eu}(\text{7})(\text{OH}_2)_2]^{3+}$ is only 1.2 kcal/mol larger than that observed for the most active mononuclear Zn(II) catalysts (Chart 1). Apparently, the larger number of donor groups to Eu(III) at $[\text{Eu}(\text{7})(\text{OH}_2)_2]^{3+}$ compared to mononuclear Zn(II) catalysts act to attenuate the 3.2 kcal/mol larger transition state stabilization that is observed for catalysis by Eu(III) when all the ligands are water. The 1.5 kcal/mol larger value of $|\Delta G_S^\ddagger|$ for $[\text{Eu}(\text{7})(\text{OH}_2)_2]^{3+}$ than for $[\text{Eu}(\text{6})(\text{OH}_2)_2]^+$ shows that there is a small increase in the catalytic efficiency with increasing total positive charge at the catalyst available to interact with the transition state dianion. Finally, the similar transition state binding energies for catalysis by $[\text{Eu}(\text{6})(\text{OH}_2)_2]^+$ and $[\text{Eu}_2(\text{6})_2(\text{OH})(\text{OH}_2)_2]^+$ provides evidence that the two metal ions at the dimeric complex operate independently in catalyzing the cleavage of **HpPNP**.

Specificity

There are significant differences in the rate accelerations for the **Zn₂(1)(H₂O)**-catalyzed cleavage of RNA analogs and a dinucleoside monophosphate that reflect the different specificities of the dinuclear complex **Zn₂(1)(H₂O)** for transition state binding (Chart 4).^{10, 11, 17, 20} The binding “site” at this catalyst has not been characterized; however, it should not show strong shape complementarity to any of these substrates. We proposed other origins for the range of transition state binding energies shown in Chart 4.

1. The difference between $\Delta G_S^\ddagger = -9.6$ and -7.2 kcal/mol for catalysis of cleavage of **HpPNP**, a minimal substrate, and of the more bulky substrate **UpPNP**, respectively, suggests that close approach of the phosphate diester to the metal cations is required for effective catalysis; and, that there is steric hindrance to the approach of the larger substrate **UpPNP** to **Zn₂(1)(H₂O)**.¹¹
2. The difference between $\Delta G_S^\ddagger = -9.3$ and -7.1 kcal/mol for catalysis of cleavage of **UpOEt** and **UpOCH₂CCl₃**, respectively, is a consequence of the different Brønsted parameters $\beta_{lg} = -1.28$ and -0.72 for the specific-base-catalyzed and **Zn₂(1)(H₂O)**-catalyzed cleavage reactions.^{17, 28} This corresponds to the neutralization of an effective transition state charge of ca. 0.56 units by interactions between the catalyst and the leaving group anion.²⁹ These data show that there is stabilization of the transition state for cleavage of **UpOEt** from interaction of the cationic catalyst with both the reacting phosphate core and with the strongly basic alkoxy leaving group.
3. The difference between $\Delta G_S^\ddagger = -9.3$ and -7.2 kcal/mol for catalysis of cleavage of **UpU** and **UpPNP**, respectively, is due partly or entirely to transition state stabilization by interaction of the catalyst with the strongly basic alkoxy leaving group at **UpU**. There may also be a weak nonspecific interaction between the catalyst and the second pyrimidine base at **UpU**.²⁰

Lessons from Studies on Small Molecule Catalysis

The high catalytic activity of **Zn₂(1)(H₂O)** arises from strong stabilizing binding interactions (ΔG_S^\ddagger , Scheme 3) between the dianionic transition state and the densely charged cationic core of **Zn₂(1)(H₂O)**.¹⁰ No concerted general base catalysis of phosphate diester cleavage is observed, presumably because anything gained from such catalysis is offset by an even larger reduction in the electrostatic stabilization of the transition state (Scheme 5).

A distinguishing feature of these metal ion complex-catalyzed reactions is their large discrimination between the binding of the substrate phosphate diester monoanion (weak), and of the oxyphosphorane-like transition state dianion³⁰ and the methyl phosphate dianion transition state analog (strong).²³ These results provide evidence that transition state stabilization by mononuclear and dinuclear metal ion complexes is due largely to electrostatic interactions, which are optimal for the dianionic transition state and transition state analog. In other words, good catalysis of the cleavage of phosphate diesters in water has been obtained relatively easily because of the intrinsically strong stabilizing interactions between densely charged metals and phosphate dianions. The total transition binding energy ΔG_S^\ddagger can be modified by interactions between the metal ion and its ligands, but these effects are small in comparison with the transition stabilization observed for catalysis by free metal ions, where the ligands are water (Chart 1).

Enzyme Catalysis

A major difference between small molecule and enzyme catalysts is that the latter have evolved mechanisms for utilization of the binding interactions between the protein and nonreacting portions of the substrate in stabilization of the transition state for the catalyzed reaction.² The

transition state binding energies of up to -10 kcal/mol observed for catalysis of the cleavage of phosphate diesters are due mainly to electrostatic interactions between the catalyst and the phosphate group, which is the reaction center. We have observed even larger transition state stabilizations of ca. 12 kcal/mol from utilization of the binding energy between enzyme catalysts and the *nonreacting* phosphodianion group of substrates for enzyme-catalyzed proton transfer, hydride transfer and decarboxylation reactions.^{31–33}

Reactions of Triosephosphates

Triosephosphate isomerase (TIM) is a prototypical catalyst of proton transfer at carbon (Chart 5). This enzyme catalyzes the stereospecific 1,2-hydrogen shift at (*R*)-glyceraldehyde 3-phosphate (**GAP**) to give dihydroxyacetone phosphate (**DHAP**). A single base (Glu-165) catalyzes suprafacial proton transfer through a *cis*-enediol(ate) intermediate.³⁴ The ratio of second-order rate constants $(k_{\text{cat}}/K_{\text{m}})_{\text{GAP}}/(k_{\text{cat}}/K_{\text{m}})_{\text{GA}} = (2.4 \times 10^8 \text{ M}^{-1} \text{ s}^{-1})/(0.34 \text{ M}^{-1} \text{ s}^{-1}) = 7 \times 10^8$ for the TIM-catalyzed isomerization of **GAP** and of (*R*)-glyceraldehyde shows that binding interactions between the enzyme and the phosphodianion group of **GAP** provide ≥ 12 kcal/mol of transition state stabilization.³⁵ This may account for all but 2 kcal/mol of the transition state stabilization for TIM-catalyzed isomerization of **GAP**.^{35,36}

The value of $(k_{\text{cat}}/K_{\text{m}})_{\text{Gly}} = 0.26 \text{ M}^{-1} \text{ s}^{-1}$ for TIM-catalyzed exchange of deuterium from solvent D_2O into the truncated substrate glycolaldehyde is similar to $(k_{\text{cat}}/K_{\text{m}})_{\text{GA}} = 0.34 \text{ M}^{-1} \text{ s}^{-1}$ for isomerization of (*R*)-glyceraldehyde.³¹ The deuterium exchange reaction of glycolaldehyde is strongly activated by addition of the second substrate “piece” phosphite dianion, HPO_3^{2-} . The data give $(k_{\text{cat}}/K_{\text{m}})_{\text{E}\cdot\text{HPi}} = 185 \text{ M}^{-1} \text{ s}^{-1}$ for turnover of glycolaldehyde by TIM that is saturated with phosphite dianion, so that binding of phosphite dianion to TIM results in a 700-fold rate acceleration of proton transfer from carbon. The two substrate pieces glycolaldehyde and HPO_3^{2-} each bind weakly to TIM and there is a large “chelate” effect for binding of the whole substrate **GAP** (Chart 5).^{31,37} The binding of HPO_3^{2-} to free TIM ($K_{\text{d}} = 38 \text{ mM}$) is 700-fold weaker than its binding to the fleeting TIM•transition state complex ($K_{\text{d}}^{\ddagger} = 53 \text{ }\mu\text{M}$, Scheme 7). This corresponds to an intrinsic phosphite dianion binding energy of -5.8 kcal/mol (Scheme 7).³¹

The proton transfer reaction catalyzed by TIM occurs in an active site at which the substrate is sequestered from solvent.^{38,39} We proposed a model for catalysis by TIM in which part of the total intrinsic binding energy of the phosphodianion group of substrate is utilized to drive a protein conformational change that sequesters the substrate at an active site with an apparent dielectric constant substantially lower than that of solvent, and with the catalytic groups optimally organized to stabilize the transition state for deprotonation of α -carbonyl carbon.^{31,40}

The whole substrate **DHAP** is reduced by NADH to give L-glycerol 3-phosphate in a reaction catalyzed by α -glycerol phosphate dehydrogenase (Scheme 8).⁴¹ The ratio $(k_{\text{cat}}/K_{\text{m}})_{\text{DHAP}}/(k_{\text{cat}}/K_{\text{m}})_{\text{Gly}} = (1 \times 10^6 \text{ M}^{-1} \text{ s}^{-1})/(0.009 \text{ M}^{-1} \text{ s}^{-1}) = 1.1 \times 10^8$ for rabbit muscle α -glycerol phosphate dehydrogenase-catalyzed reduction of **DHAP** and glycolaldehyde gives an intrinsic phosphate binding energy of -11 kcal/mol, which is similar to that for TIM.³³ We find that phosphite dianion is also a powerful activator of enzyme-catalyzed reduction of the truncated neutral substrate glycolaldehyde by NADH.³³ X-ray crystallographic analysis of human α -glycerol phosphate dehydrogenase provides evidence that the phosphate binding energy of the substrate is used to *drive* the closure of a loop over the substrate.⁴¹

Orotidine 5'-Monophosphate Decarboxylase (OMPDC)

OMPDC is a remarkable enzyme that effects an enormous 10^{17} -fold acceleration of the chemically very difficult decarboxylation of orotidine 5'-monophosphate (**OMP**, Chart 6) to

give uridine 5'-monophosphate (UMP).⁴² The enzymatic⁴³ and nonenzymatic⁴⁴ decarboxylation reactions proceed through the vinyl carbanion intermediates. Comparison of the X-ray crystal structures of free yeast OMPDC and that complexed with the transition state analog 6-hydroxyuridine 5'-monophosphate shows that ligand binding results in a large motion to “close” the active site, with the formation of numerous protein-ligand contacts, including five hydrogen bonds to the phosphodianion group.⁴⁵ The phosphodianion at **OMP**, or at any phosphorylated enzymatic substrate, may simply “anchor” the substrate to the enzyme, or the enzyme conformational change effected by the small remote group may directly assist in the creation of an active site that provides optimal transition state stabilization.

The intrinsic binding energy of the phosphodianion group of **OMP**, calculated from the ratio of second-order rate constants k_{cat}/K_m for the OMPDC-catalyzed reactions of **OMP** ($9.4 \times 10^6 \text{ M}^{-1} \text{ s}^{-1}$)⁴⁶ and the truncated substrate 1-(β -D-erythrofuransyl)orotic acid (**EO**, $2.1 \times 10^{-2} \text{ M}^{-1} \text{ s}^{-1}$)³² is -12 kcal/mol (Chart 6). The weak binding of the **EO** ($K_d \approx 0.1 \text{ M}$) and phosphite dianion ($K_d = 0.14 \text{ M}$) pieces to OMPDC is striking, in view of the tight binding of the whole substrate **OMP** ($K_m = 1.6 \mu\text{M}$).^{37,46} Decarboxylation of **EO** is strongly activated by phosphite dianion, with $(k_{\text{cat}}/K_m)_{\text{E} \cdot \text{HPi}} = 1600 \text{ M}^{-1} \text{ s}^{-1}$ for turnover of **EO** by OMPDC that is saturated with HPO_3^{2-} , so that the binding of this dianion to OMPDC results in an 80,000-fold acceleration of decarboxylation.³² The binding of HPO_3^{2-} to OMPDC ($K_d = 0.14 \text{ M}$) must also be 80,000-fold weaker than its binding to the fleeting complex of OMPDC with **EO** in the transition state ($K_d^\ddagger = 1.8 \mu\text{M}$, Scheme 7). The total intrinsic binding energy of HPO_3^{2-} at the transition state complex is therefore -7.8 kcal/mol . This is divided into the small -1.2 kcal/mol binding energy observed in the ground state complex, and an additional -6.6 kcal/mol interaction that develops on proceeding to the transition state for enzyme-catalyzed decarboxylation of **EO**.^{2,32}

The Pauling Paradigm

Our studies have shown that the interactions between nonreacting phosphodianion fragments of substrate and the protein provide an 11–12 kcal/mol stabilization of the transition states for proton transfer, hydride transfer and decarboxylation reactions. Therefore, enzymes that catalyze the reactions of small phosphorylated substrates such as **GAP** and **DHAP** have a potential transition state binding energy of -12 kcal/mol . The medium-sized phosphorylated substrate **OMP** interacts with OMPDC via its phosphodianion, ribose sugar ring and nucleic acid base portions, and exhibits a transition state binding energy far in excess of -15 kcal/mol that was proposed as the limit on noncovalent enzyme catalysis.^{3,42}

Pyridoxal 5'-phosphate (PLP) provides impressive covalent catalysis of the deprotonation of α -amino acids to form α -amino carbanions.⁴⁷ However, the large rate acceleration for proton transfer obtained by recruitment of this cofactor can be also obtained by protein catalysts, such as proline racemase. This enzyme provides a 19 kcal/mol stabilization of the transition state for deprotonation of enzyme-bound proline by interaction with the protein catalyst.⁴⁸ Our proposal that “pure protein catalysis” of deprotonation of amino acids results from the binding of the amino acid substrate at a nonpolar active site that favors formation of a carbanion zwitterion^{49,50} has been supported by X-ray crystallographic and computational studies.^{51, 52} We are generally skeptical of arguments that cofactors such as PLP have evolved to do what is impossible for protein catalysts, because of the great diversity of protein-catalyzed reactions. On the other hand, cofactor-catalysis is often simpler and more general than protein catalysis, and these factors favor the recruitment of cofactors in enzymatic catalysis.

Acknowledgements

We acknowledge the NSF (CHE0415356) and the NIH (GM39754) for support of our work, and we thank our coworkers named in the references for their many contributions to our research.

References

1. Pauling L. The nature of forces between large molecules of biological interest. *Nature* 1948;161:707–709. [PubMed: 18860270]
2. Jencks WP. Binding energy, specificity and enzymic catalysis: the circe effect. *Adv Enzymol Relat Areas Mol Biol* 1975;43:219–410. [PubMed: 892]
3. Zhang X, Houk KN. Why enzymes are proficient catalysts: beyond the Pauling paradigm. *Acc Chem Res* 2005;38:379–385. [PubMed: 15895975]
4. Morrow J, Iranzo O. Synthetic metallonucleases for RNA cleavage. *Curr Opin Chem Biol* 2004;8:192–200. [PubMed: 15062781]
5. Williams NH, Takashi B, Wall M, Chin J. Structure and nuclease activity of simple dinuclear metal complexes: quantitative dissection of the role of metal ions. *Acc Chem Res* 1999;32:485–493.
6. Blasko A, Bruice TC. Recent studies of nucleophilic, general-acid and metal ion catalysis of phosphate diester hydrolysis. *Acc Chem Res* 1999;32:475–484.
7. Chin KOA, Morrow JR. RNA cleavage and phosphate diester transesterification by encapsulated lanthanide ions: traversing the lanthanide series with lanthanum(III), europium(III), and lutetium(III) complexes of 1,4,7,10-tetrakis(2-hydroxyalkyl)-1,4,7,10 tetraazacyclododecane. *Inorg Chem* 1994;33:5036–5041.
8. Morrow JR, Buttrey LA, Shelton VM, Berback KA. Efficient catalytic cleavage of RNA by lanthanide (III) macrocyclic complexes: toward synthetic nucleases for *in vivo* applications. *J Am Chem Soc* 1992;114:1903–1905.
9. Baker BF, Khalili H, Wei N, Morrow JR. Cleavage of the 5' cap structure of *mRNA* by a europium (III) macrocyclic complex with pendant alcohol group. *J Am Chem Soc* 1997;119:8749–8755.
10. Iranzo O, Kovalevsky AY, Morrow JR, Richard JP. Physical and kinetic analysis of the cooperative role of metal ions in catalysis of phosphodiester cleavage by a dinuclear Zn(II) complex. *J Am Chem Soc* 2003;125:1988–1993. [PubMed: 12580627]
11. Yang M-Y, Richard JP, Morrow JR. Substrate specificity for catalysis of phosphodiester cleavage by a dinuclear Zn(II) complex. *Chem Commun* 2003:2832–2833.
12. Yang MY, Iranzo O, Richard JP, Morrow JR. Solvent deuterium isotope effects on phosphodiester cleavage catalyzed by an extraordinarily active Zn(II) complex. *J Am Chem Soc* 2005;127:1064–1065. [PubMed: 15669821]
13. Voss DA, Farquhar ER, WDHorrock J, Morrow JR. Lanthanide(III) complexes of an amide derivative of DOTA exhibit an unusual variation in stability across the lanthanide series. *Inorg Chim Acta* 2004;859–863.
14. Iranzo O, Richard JP, Morrow JR. Structure-activity studies on the cleavage of an RNA analog by a potent dinuclear metal ion catalyst. The effect of changing the metal ion. *Inorg Chem* 2004;43:1743–1750. [PubMed: 14989667]
15. Iranzo O, Elmer T, Richard JP, Morrow JR. Cooperativity between metal ions in the cleavage of phosphate diesters and RNA by dinuclear Zn(II) catalysts. *Inorg Chem* 2003;42:7737–7746. [PubMed: 14632489]
16. Farquhar E, Richard JP, Morrow JR. Formation and stability of mononuclear and dinuclear Eu(III) complexes and their catalytic reactivity toward cleavage of an RNA analog. *Inorg Chem* 2007;46:7169–7177. [PubMed: 17655292]
17. Yang, M-Y. PhD Thesis. University at Buffalo; 2007.
18. Mathews RA, Rossiter CS, Morrow JR, Richard JP. A minimalist approach to understanding the efficiency of mononuclear Zn(II) complexes as catalysts of cleavage of an RNA analog. *J Chem Soc, Dalton Trans* 2007:3804–3811.
19. Nwe K, Richard JP, Morrow JR. Direct excitation luminescence spectroscopy of Eu(III) complexes of 1,4,7-tris(carbamoylmethyl)-1,4,7,10- tetraazacyclododecane derivatives and kinetic studies of their catalytic cleavage of an RNA analog. *J Chem Soc, Dalton Trans* 2007:5171–5178.
20. O'Donoghue A, Pyun SY, Yang MY, Morrow JR, Richard JP. Substrate specificity of an active dinuclear complex for cleavage of RNA analogs and a dinucleoside. *J Am Chem Soc* 2006;128:1615–1621. [PubMed: 16448134]

21. Feng G, Mareque-Rivas JC, Martin de Rossales RT, Williams NH. A highly reactive mononuclear Zn(II) complex for phosphodiester cleavage. *J Am Chem Soc* 2005;128:13470–13471. [PubMed: 16190690]
22. Neverov AA, Lu ZL, Maxwell CI, Mohamed MF, White CJ, Tsang JSW, Brown RS. Combination of a dinuclear Zn²⁺ complex and a medium effect exerts a 10¹²-fold rate enhancement of cleavage of an RNA and DNA model system. *J Am Chem Soc* 2006;128:16398–16405. [PubMed: 17165797]
23. Yang MY, Morrow JR, Richard JP. A transition state analog for phosphate diester cleavage catalyzed by a small enzyme-like metal ion complex. *Bioorg Chem* 2007;35:366–374. [PubMed: 17434205]
24. Wolfenden R. Transition state analogues for enzyme catalysis. *Nature* 1969;223:704–705. [PubMed: 4979456]
25. Crueiras J, Richard JP. A comparison of the electrophilic reactivities of Zn²⁺ and acetic acid as catalysts of enolization: imperatives for enzymatic catalysis of proton transfer at carbon. *J Am Chem Soc* 2004;126:5164–5173. [PubMed: 15099099]
26. Nagorski RW, Richard JP. Mechanistic imperatives for aldose-ketose isomerization in water: specific-, general base- and metal ion-catalyzed isomerization of glyceraldehyde with proton and hydride transfer. *J Am Chem Soc* 2001;123:794–802. [PubMed: 11456612]
27. Fry FH, Moubaraki B, Murray KS, Spiccia L, Warren M, Skelton BW, White AH. Asymmetry in endogenously bridged binuclear copper(II) and zinc(II) complexes formed by 1,2-bis[1,4,7-triazacyclonon-1-yl]-propan-2-ol. *J Chem Soc, Dalton Trans* 2003:866–871.
28. Kosonen M, Youseti-Salakdeh E, Stromberg R, Lönnberg H. Mutual isomerization of uridine 2'- and 3'-alkylphosphates and cleavage to a 2',3'-cyclic phosphate: the effect of the alkyl group on the hydronium- and hydroxide-ion-catalyzed reactions. *J Chem Soc, Perkin Trans* 1997;2:2661–2666.
29. Williams A. Electronic charge and transition state structure in solution. *Adv Phys Org Chem* 1992;27:1–55.
30. Perreault DM, Anslyn EV. Unifying the current data on the mechanism of cleavage-transesterification of RNA. *Angew Chem, Int Ed Engl* 1997;36:432–450.
31. Amyes TL, Richard JP. Enzymatic catalysis of proton transfer at carbon: activation of triosephosphate isomerase by phosphite dianion. *Biochemistry* 2007;46:5841–5854. [PubMed: 17444661]
32. Amyes TL, Richard JP, Tait JJ. Activation of orotidine 5'-monophosphate decarboxylase by phosphite dianion: the whole substrate is the sum of two parts. *J Am Chem Soc* 2005;127:15708–15709. [PubMed: 16277505]
33. Tsang W-Y, Amyes TL, Richard JP. Manuscript in preparation
34. Knowles JR, Alberly WJ. Perfection in enzyme catalysis: the energetics of triosephosphate isomerase. *Acc Chem Res* 1977;10:105–111.
35. Amyes TL, O'Donoghue AC, Richard JP. Contribution of phosphate intrinsic binding energy to the enzymatic rate acceleration for triosephosphate isomerase. *J Am Chem Soc* 2001;123:11325–11326. [PubMed: 11697989]
36. Richard JP. Acid-base catalysis of the elimination and isomerization reactions of triose phosphates. *J Am Chem Soc* 1984;106:4926–4936.
37. Jencks WP. On the attribution and additivity of binding energies. *Proc Natl Acad Sci U S A* 1981;78:4046–4050. [PubMed: 16593049]
38. O'Donoghue AC, Amyes TL, Richard JP. Hydron transfer catalyzed by triosephosphate isomerase. Products of isomerization of (*R*)-glyceraldehyde 3-phosphate in D₂O. *Biochemistry* 2005;44:2610–2621. [PubMed: 15709774]
39. O'Donoghue AC, Amyes TL, Richard JP. Hydron transfer catalyzed by triosephosphate isomerase. Products of isomerization of dihydroxyacetone phosphate in D₂O. *Biochemistry* 2005;44:2622–2631. [PubMed: 15709775]
40. Sampson NS, Knowles JR. Segmental motion in catalysis: investigation of a hydrogen bond critical for loop closure in the reaction of triosephosphate isomerase. *Biochemistry* 1992;31:8488–8494. [PubMed: 1390633]
41. Ou X, Ji C, Han X, Zhao X, Li X, Mao Y, Wong LL, Bartlam M, Rao Z. Crystal structure of human glycerol 3-phosphate dehydrogenase (GPDH). *J Mol Biol* 2006;357:858–869. [PubMed: 16460752]
42. Radzicka A, Wolfenden R. A proficient enzyme. *Science* 1995;267:90–93. [PubMed: 7809611]

43. Toth K, Amyes TL, Wood BM, Chan K, Gerlt JA, Richard JP. Product deuterium isotope effect for orotidine 5'-monophosphate decarboxylase: evidence for the existence of a short-lived carbanion intermediate. *J Am Chem Soc* 2007;129:12946–12947. [PubMed: 17918849]
44. Sievers A, Wolfenden R. Equilibrium of formation of the 6-carbanion of UMP, a potential intermediate in the action of OMP decarboxylase. *J Am Chem Soc* 2002;124:13986–13987. [PubMed: 12440884]
45. Miller BG, Hassell AM, Wolfenden R, Milburn MV, Short SA. Anatomy of a proficient enzyme: the structure of orotidine 5'-monophosphate decarboxylase in the presence and absence of a potential transition state analog. *Proc Natl Acad Sci U S A* 2000;97:2011–2016. [PubMed: 10681417]
46. Porter DJT, Short SA. Yeast orotidine-5'-phosphate decarboxylase: steady-state and pre-steady-state analysis of the kinetic mechanism of substrate decarboxylation. *Biochemistry* 2000;39:11788–11800. [PubMed: 10995247]
47. Toth K, Richard JP. Covalent catalysis by pyridoxal: evaluation of the effect of the cofactor on the carbon acidity of glycine. *J Am Chem Soc* 2007;129:3013–3021. [PubMed: 17298067]
48. Williams G, Maziarz EP, Amyes TL, Wood TD, Richard JP. Formation and stability of the enolates of N-protonated proline methyl ester and proline zwitterion in aqueous solution: a nonenzymatic model for the first step in the racemization of proline catalyzed by proline racemase. *Biochemistry* 2003;42:8354–8361. [PubMed: 12846584]
49. Rios A, Amyes TL, Richard JP. Formation and stability of organic zwitterions in aqueous solution: enolates of the amino acid glycine and its derivatives. *J Am Chem Soc* 2000;122:9373–9385.
50. Richard JP, Amyes TL. On the importance of being zwitterionic: enzymic catalysis of decarboxylation and deprotonation of cationic carbon. *Bioorg Chem* 2004;32:354–366. [PubMed: 15381401]
51. Puig E, Garcia-Viloca M, Gonzalez-Lafont A, Lluch JM. On the ionization state of the substrate in the active site of glutamate racemase. A QM/MM study about the importance of being zwitterionic. *J Phys Chem A* 2006;110:717–725. [PubMed: 16405345]
52. Pillai B, Cherney MM, Diaper CM, Sutherland A, Blanchard JS, Vereras JC, James MNG. Structural insights into stereochemical inversion by diaminopimilate epimerase: an antibacterial drug target. *Proc Natl Acad Sci U S A* 2006;103:8668–8673. [PubMed: 16723397]

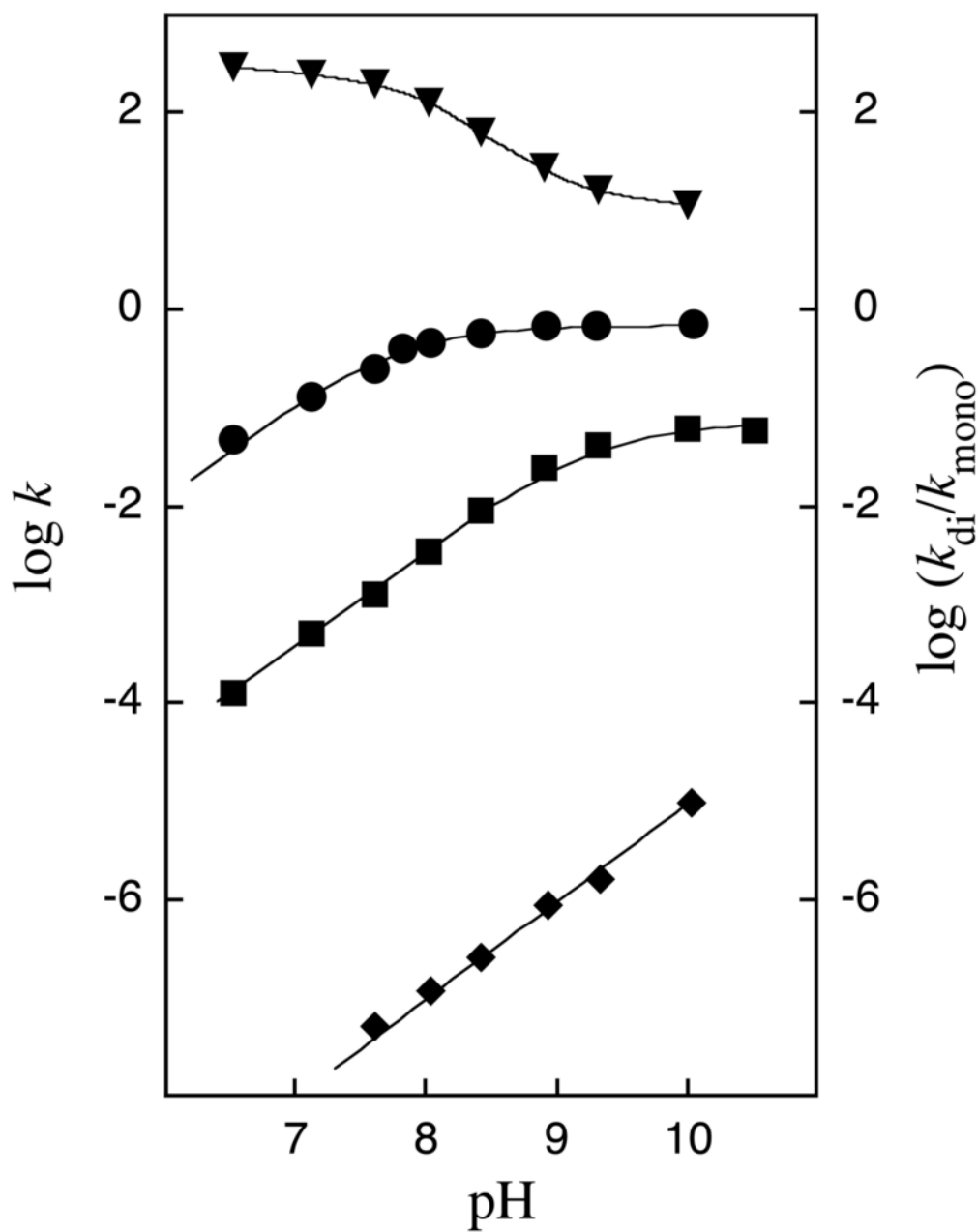
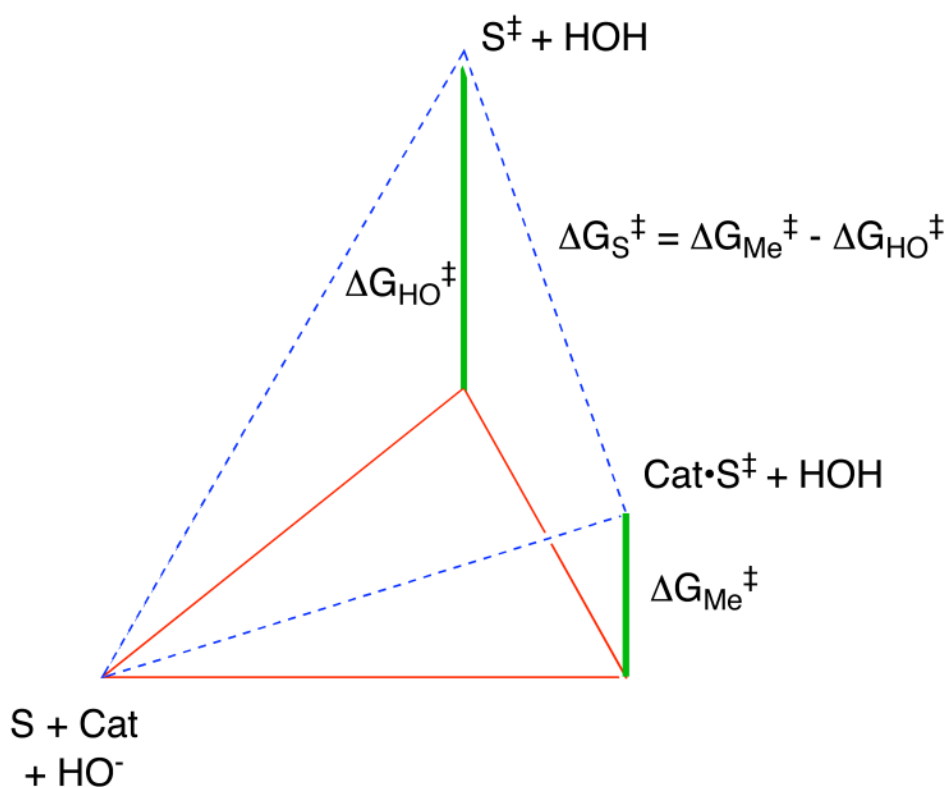
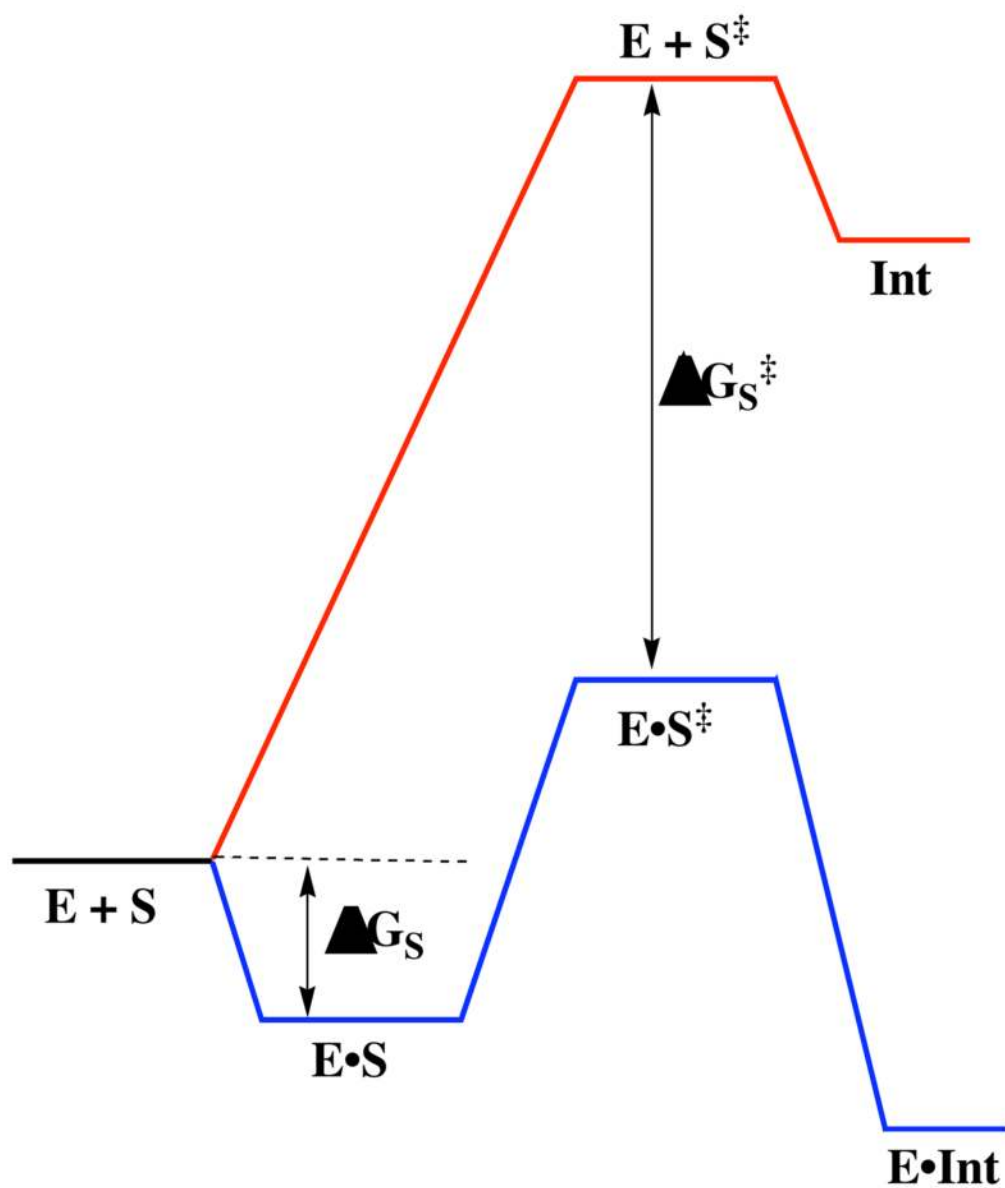


Figure 1.

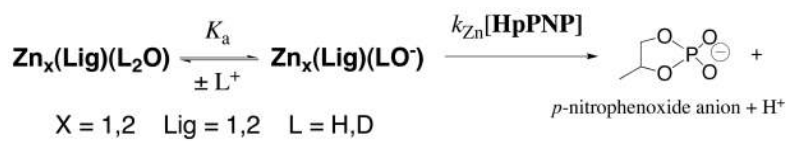
pH-rate profiles for cleavage of **HpPNP** catalyzed by HO^- and $\text{Zn}(\text{II})$ complexes in water at 25°C .¹⁰ Key: (\blacklozenge), k_{obsd} (s^{-1}) for spontaneous HO^- -catalyzed cleavage; (\blacksquare), k_{Me} ($\text{M}^{-1} \text{s}^{-1}$) for cleavage catalyzed by **Zn(2)(H₂O)**; (\bullet), k_{Me} ($\text{M}^{-1} \text{s}^{-1}$) for cleavage catalyzed by **Zn₂(1)(H₂O)**; (\blacktriangledown), ratio of k_{Me} for cleavage catalyzed by the dinuclear (k_{di}) and mononuclear (k_{mono}) $\text{Zn}(\text{II})$ complexes.

**Figure 2.**

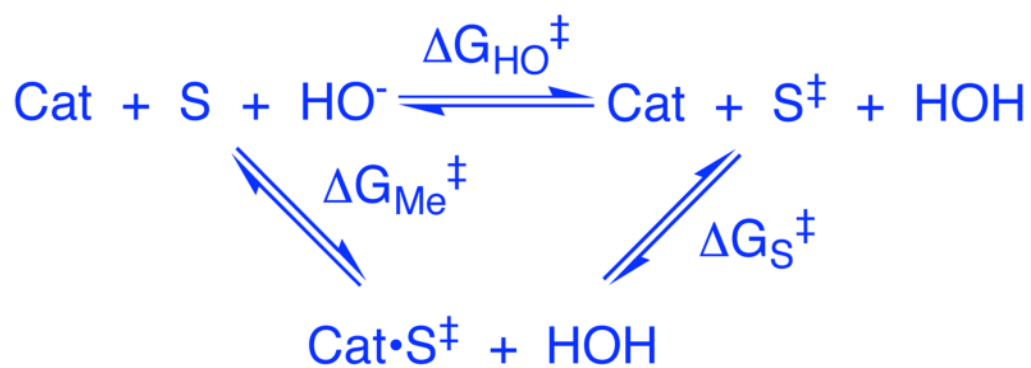
Bar graph which shows the barrier for HO^{-} -promoted phosphate diester cleavage in water ($\Delta G_{HO^{\ddagger}}$, green bar), the barrier for the metal ion complex-catalyzed hydroxide ion-promoted reaction ($\Delta G_{Me^{\ddagger}}$, green bar), and the binding energy for the transition state for the aqueous HO^{-} -promoted reaction ($\Delta G_{S^{\ddagger}}$).



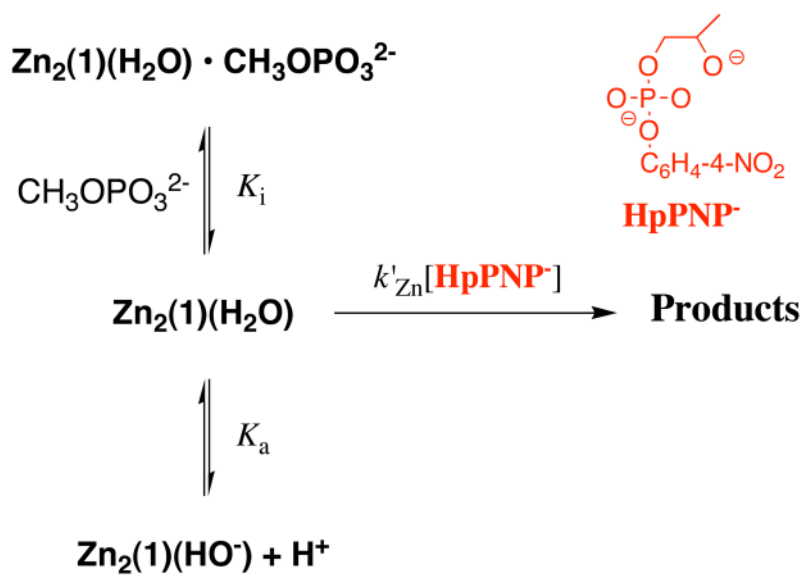
Scheme 1.



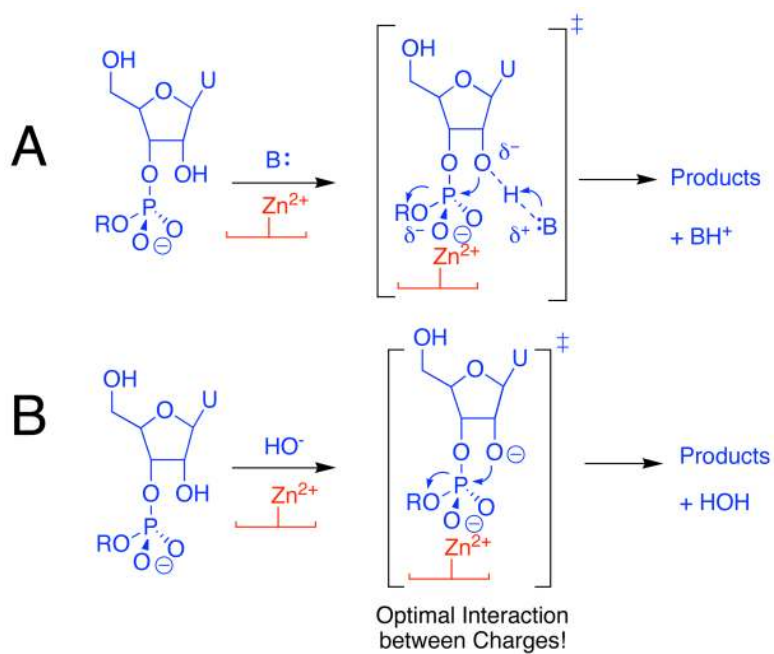
Scheme 2.



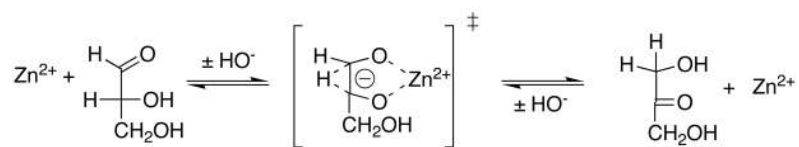
Scheme 3.



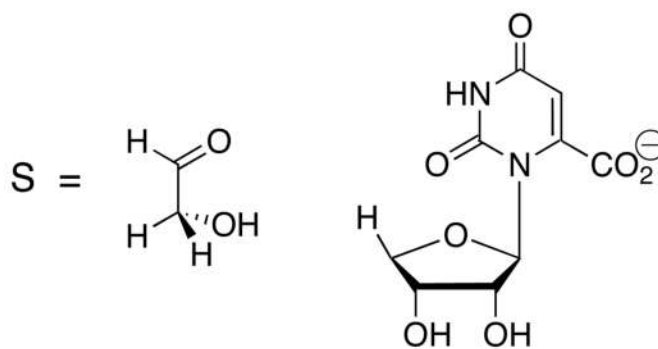
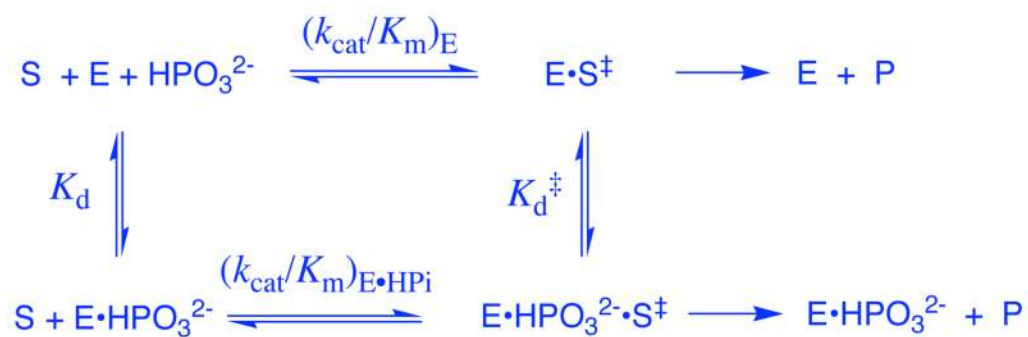
Scheme 4.



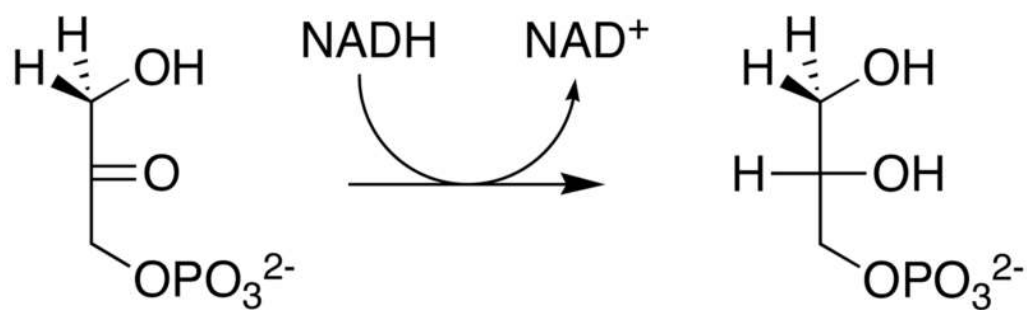
Scheme 5.



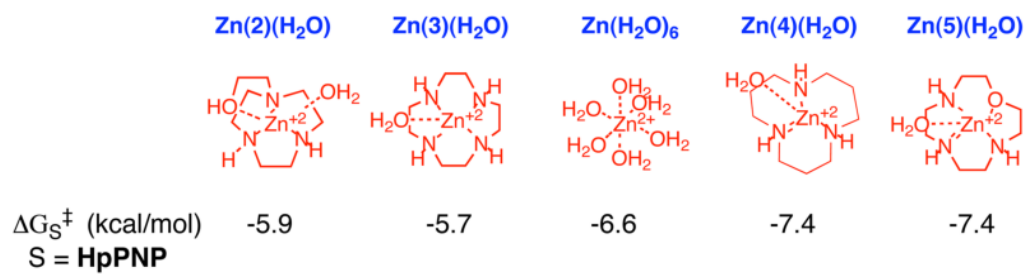
Scheme 6.



Scheme 7.



Scheme 8.

**Chart 1.**

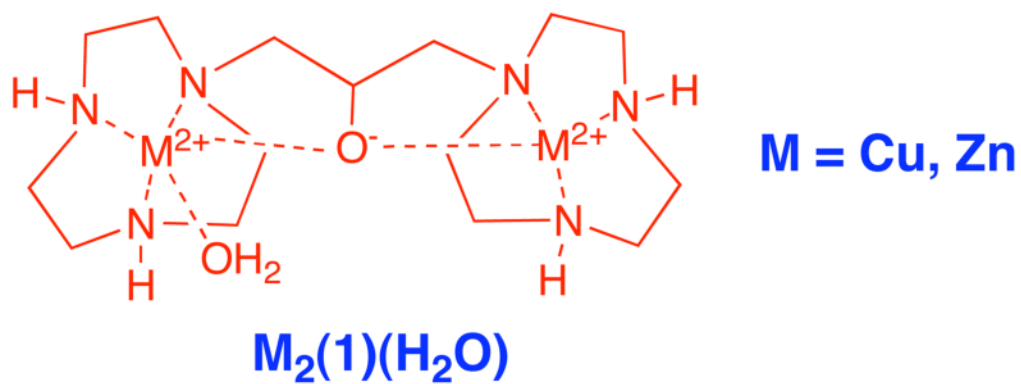


Chart 2.

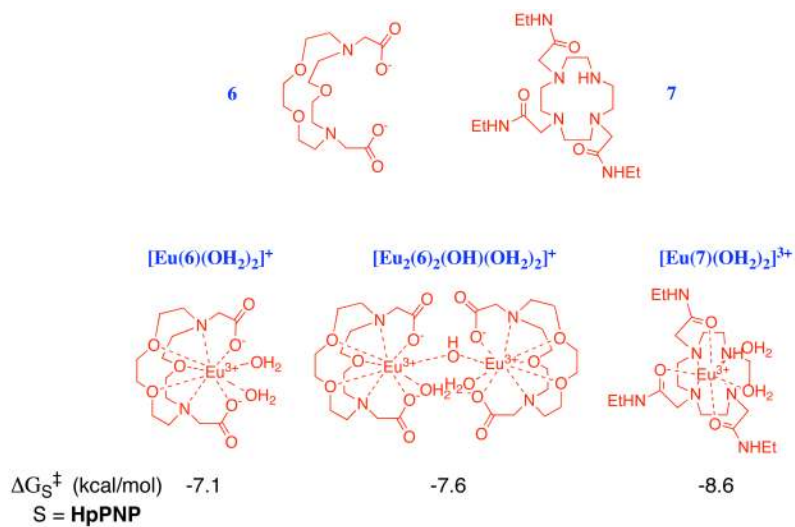


Chart 3.

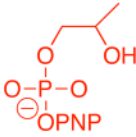
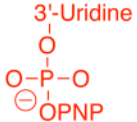
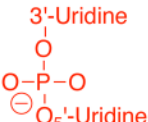
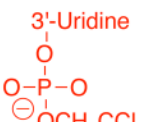
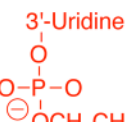
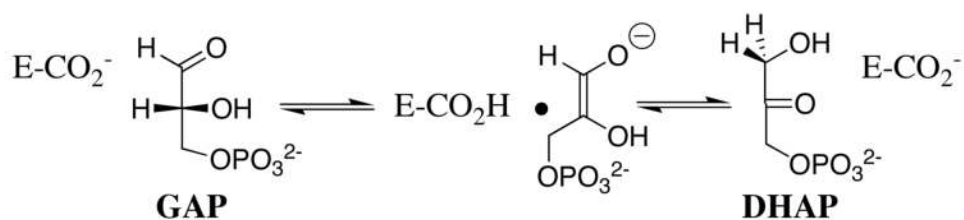
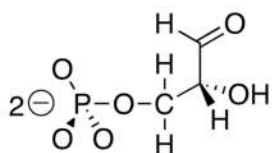
	HpPNP	UpPNP	UpU	UpOCH ₂ CCl ₃	UpOEt
					
ΔG_S^\ddagger (kcal/mol)	-9.6	-7.2	-9.3	-7.1	-9.3
Cat = Zn₂(1)(H₂O)					

Chart 4.

Triosephosphate Isomerase



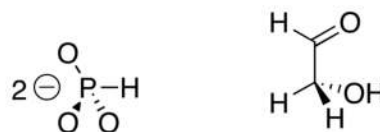
Holistic Substrate



$$K_m = 1.8 \times 10^{-5} \text{ M}$$

$$k_{\text{cat}}/K_m = 2.4 \times 10^8 \text{ M}^{-1} \text{ s}^{-1}$$

Two-Part Substrate



$$K_d = 3.8 \times 10^{-2} \text{ M} \quad K_d > 2 \times 10^{-3} \text{ M}$$

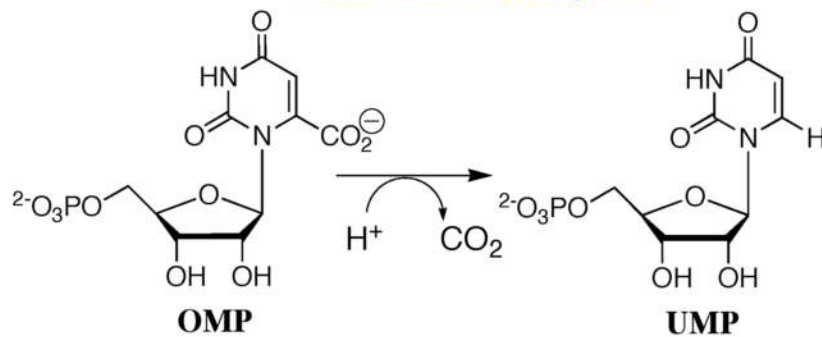
$$(k_{\text{cat}}/K_m)_E = 0.26 \text{ M}^{-1} \text{ s}^{-1}$$

$$(k_{\text{cat}}/K_m)_{E\bullet\text{HPi}} = 185 \text{ M}^{-1} \text{ s}^{-1}$$

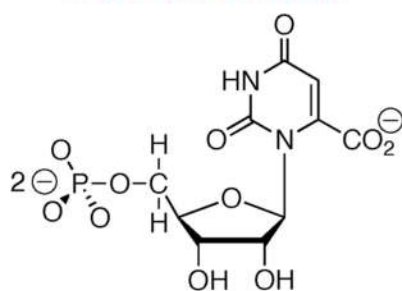
700-fold activation by the binding of phosphite dianion

Chart 5.

OMP Decarboxylase



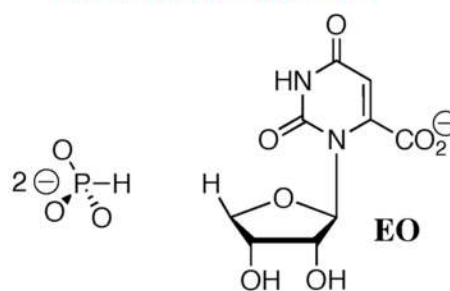
Holistic Substrate



$$K_m = 1.6 \times 10^{-6} \text{ M}$$

$$k_{\text{cat}}/K_m = 9.4 \times 10^6 \text{ M}^{-1} \text{ s}^{-1}$$

Two-Part Substrate



$$K_d = 0.14 \text{ M} \quad K_d \approx 0.1 \text{ M}$$

$$(k_{\text{cat}}/K_m)_E = 2.1 \times 10^{-2} \text{ M}^{-1} \text{ s}^{-1}$$

$$(k_{\text{cat}}/K_m)_{E \cdot \text{HPi}} = 1600 \text{ M}^{-1} \text{ s}^{-1}$$

80,000-fold activation by the binding of phosphite dianion

Chart 6.